nature cell biology

c-Myc binds to human ribosomal DNA and stimulates transcription of rRNA genes by RNA polymerase I

Carla Grandori[1,3,4], Natividad Gomez-Roman[2], Zoe A. Felton-Edkins[2], Celine Ngouenet[3], Denise A. Galloway[1], Robert N. Eisenman[3] and Robert J.White[2]

c-Myc coordinates cell growth and division through a transcriptional programme that involves both RNA polymerase (Pol) II- and Pol III-transcribed genes. Here, we demonstrate that human c-Myc also directly enhances Pol I transcription of ribosomal RNA (rRNA) genes. rRNA synthesis and accumulation occurs rapidly following activation of a conditional *MYC-ER* allele (coding for a Myc–oestrogen-receptor fusion protein), is resistant to inhibition of Pol II transcription and is markedly reduced by *c-MYC* RNA interference. Furthermore, by using combined immunofluorescence and rRNA-FISH, we have detected endogenous c-Myc in nucleoli at sites of active ribosomal DNA (rDNA) transcription. Our data also show that c-Myc binds to specific consensus elements located in human rDNA and associates with the Pol I-specific factor SL1. The presence of c-Myc at specific sites on rDNA coincides with the recruitment of SL1 to the rDNA promoter and with increased histone acetylation. We propose that stimulation of rRNA synthesis by c-Myc is a key pathway driving cell growth and tumorigenesis.

Production of ribosomal RNA (rRNA) is a fundamental step in ribosome biogenesis and in determining the protein synthesis capacity of the cell. Pol I is uniquely responsible for rRNA gene transcription (for a review, see ref. 1). The rate of rRNA transcription is highly responsive to the cellular demand for protein synthesis, being stimulated during cell-cycle entry and progression, or downregulated in response to deprivation of nutrients or growth factors.

c-Myc is an essential protein that coordinates a transcriptional programme driving cell growth and division (for reviews, see refs 2,3). Deregulated overexpression of c-Myc leads to cancer[4]. c-Myc expression is induced by extracellular signals that trigger the G0/G1 transition. Its expression is necessary and sufficient for cell-cycle entry as activation of a conditional *MYC-ER* allele in low amounts of serum promotes cell-cycle entry and growth[5]. c-Myc has also been shown to drive of cell growth in *Drosophila melanogaster*, in which loss-of-function mutations in dMyc result in reduced cell and organ size[6]. Similarly, tissue-specific deletions of c-Myc and N-Myc (neuronal Myc) in mice and in cell lines leads to decreased cell growth and proliferation[7–9]. By contrast, dMyc overexpression in *D. melanogaster* or c-Myc in mammalian cells can lead to a prominent increase in nuclear, nucleolar and overall cell size[6,10–12].

But what is the mechanism underlying the profound effects of c-Myc on cell growth? Expression array and proteomic studies[13–16], as well as analyses of c-Myc DNA binding sites[17,18], indicate that c-Myc transcriptionally regulates a wide range of Pol II-transcribed genes, including ribosomal protein genes, that are involved in metabolism and protein biosynthesis. In addition, c-Myc interacts with the Pol III transcription apparatus to enhance transcription of transfer RNAs (tRNAs), 5S rRNA and a subset of other small RNA genes[19]. The broad stimulation of translation-related genes raised the question of whether c-Myc might also cooperate with Pol I to coordinate the synthesis of rRNA with ribosomal protein and translational components that are generated by Pol II and Pol III. Expression of c-Myc correlates with increased synthesis of rRNAs and their precursors, as indicated by labelling c-Myc-overexpressing primary human fibroblasts with ^{3}H-uridine or with ^{3}H-methylmethionine (Fig. 1a–c). This effect was not obtained using wild-type or mutant versions of the nucleolar RNA helicase DDX18 (ref. 20), which is implicated in rRNA processing (C.G., unpublished observations). A marked increase in the steady-state levels of mature rRNAs in cells overexpressing c-Myc was also observed (Fig. 1b,c).

To more directly determine if induction of c-Myc stimulates Pol-I transcription, we used the human B cell line P-493-6, which carries a tetracycline-regulated *c-MYC* gene[11]. Reverse transcription PCR (RT-PCR) analysis showed increased expression of the 45S pre-rRNA when c-Myc was induced by the removal of tetracycline (Fig. 1d). The primers used for pre-rRNA recognize the 5′-external transcribed spacer (5′-ETS), which is processed rapidly during transcription and therefore reflects the rate of Pol-I transcription initiation. An increase in rRNA transcription, within 4 h of tetracycline withdrawal, was confirmed by nuclear run-on assays using the 5′-ETS and 28S coding regions of rRNA genes (Fig. 1e), whereas no change was observed with probes for Max and the tubulin

[1]Division of Human Biology, Fred Hutchinson Cancer Research Center, Seattle, WA 98109-1024, USA. [2]Institute of Biomedical and Life Sciences, Division of Biochemistry and Molecular Biology, University of Glasgow, Glasgow G12 8QQ, UK. [3]Division of Basic Sciences, Fred Hutchinson Cancer Research Center, Seattle, WA 98109-1024, USA.
[4]Correspondence should be addressed to C.G. (e-mail: cgrandor@fhcrc.org)

Published online: 20 February 2005 DOI: 10.1038/ncb1224

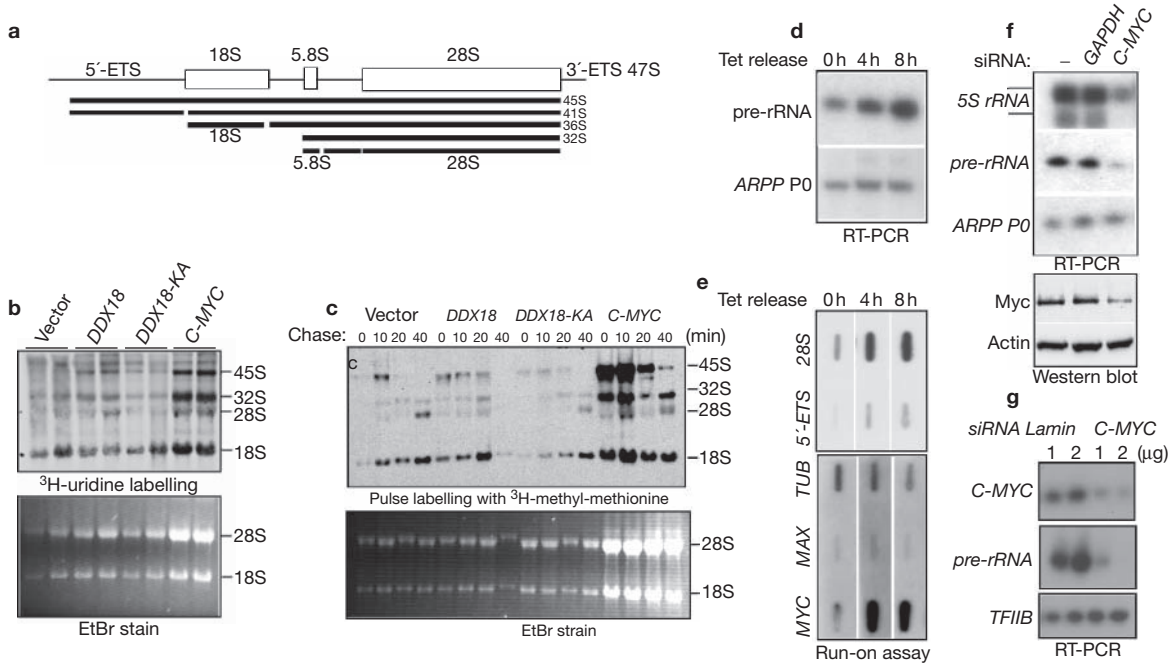

Figure 1 rRNA synthesis responds to c-Myc levels. (**a**) Schematic diagram of mammalian rRNA processing from the large 47S precursor[34]. (**b**) Detection of pre-rRNA synthesis by ^{3}H-uridine in human primary fibroblasts (WI38) transduced by retroviruses expressing c-Myc and, for comparison, the DDX18 RNA helicase and a dominant-negative mutant DDX18-KA, shown in duplicates[20]. Pre-rRNAs, normalized by cell number, were analysed by northern blots and autoradiography. Total rRNA was visualized by ethidium bromide staining (EtBr). (**c**) Pre-rRNA synthesis and processing monitored by pulse labeling with ^{3}H-methyl-methionine in cells, as in b. (**d**) Reverse transcription PCR (RT-PCR) analysis of pre-rRNA and ARPP P0 mRNA in P-493-6 cells at the indicated times after c-Myc induction by tetracycline (Tet) release. (**e**) Nuclear run-on assays showing transcription of the 5′-ETS and 28S-coding regions of rRNA genes, as well as *MYC*, *MAX* and tubulin (*TUB*) genes, in P-493-6 cells at the indicated times after c-Myc induction by tetracycline release. (**f**) RT-PCR analysis of 5S rRNA, pre-rRNA and ARPP P0 mRNA from growing HeLa cells transfected with 50 nM siRNAs against c-Myc or glyceraldehyde-3-phosphate dehydrogenase (control). Western blots confirm the specific downregulation of c-Myc but not actin. (**g**) RT-PCR analysis of c-Myc mRNA, pre-rRNA and TFIIB mRNA from growing HeLa cells transfected with 1 μg or 2 μg (as indicated) of pSUPER vectors encoding siRNAs against *C-MYC* or lamin (control).

gene TUB. These results indicate that c-Myc overexpression stimulates the transcription of rRNA genes in vivo. RNA interference was used to determine whether or not pre-rRNA synthesis is sensitive to the level of endogenous c-Myc. RT-PCR showed that pre-rRNA expression is decreased significantly by c-Myc depletion from HeLa cells using two different small interfering RNAs (siRNAs; Fig. 1f,g). Specificity is indicated by the lack of effect of siRNAs against glyceraldehyde-3-phosphate dehydrogenase (GAPDH) or lamin. As predicted[19], c-Myc depletion also reduces 5S rRNA expression by Pol III, but does not affect negative-control mRNAs encoding TFIIB or ARPP P0. Titration of siRNAs indicated that reduction of pre-rRNA is dose dependent (Fig. 1g, and see Supplementary Information, Fig. S1).

To determine whether or not c-Myc activates Pol I transcription directly, we monitored pre-rRNA synthesis in fibroblasts during induction of a conditional *MYC-ER* allele[21]. Activation of Myc-ER with 4-hydroxy-tamoxifen (4-OHT) led to a rapid increase in pre-rRNA synthesis that was resistant to the Pol II inhibitor α-amanitin (Fig. 2a), showing that Myc-ER is not enhancing rRNA transcription as a secondary response mediated by Pol II. Also, the *Δ-MYC-ER* mutant allele that was deleted in the transactivation domain (Fig. 2a) had no effect. Accumulation of full-length rRNA precursors was also demonstrated by in vivo labelling with ^{3}H-uridine following a time course of Myc-ER activation in quiescent human fibroblasts that had been exposed to 4-OHT (Fig. 2b). rRNA synthesis was evident 3–4 h after Myc-ER activation, but not in cells that had been transduced with Δ-Myc-ER or with an empty retroviral vector. Myc-ER-expresing cells also accumulate higher levels of processed rRNAs (28S, 18S and 5.8S). The increased pre-rRNA synthesis in the Myc-ER-expressing cells is also resistant to treatment with α-amanitin (see Supplementary Information, Fig. S1b). The low levels of rRNA synthesis in the controls reflects the fact that the cells were quiescent, whereas the increased baseline levels in the Myc-ER sample is due to leakiness of the Myc-ER. The rapid increase of rRNA synthesis following Myc-ER activation and its resistance to α-amanitin strongly indicates that c-Myc affects the Pol I transcription machinery directly. Furthermore, induction of Pol I transcription could be mimicked *in vitro* using an rRNA gene plasmid and nuclear extracts prepared from Myc-ER-transduced murine fibroblasts that had been treated with 4-OHT (Fig. 2c).

Human rRNA genes are organized into clusters of ~43 kb repeats that are distributed among different chromosomes[22]. These gene clusters then colocalize in the nucleolus, where rRNA synthesis and processing occurs. We examined c-Myc subcellular localization in human fibroblasts during the G0/G1 transition, a phase of the cell cycle when c-Myc expression peaks and when rRNA transcription increases. Although little, if any, c-Myc-specific signal is detected in quiescent cells, within a few hours after serum addition discrete c-Myc foci are detected throughout the nucleus, including the nucleolus. This was indicated using wide-field epi-flourescence deconvolution microscopy (DeltaVision) of cells that had been doubly stained with the nucleolar marker Mab 1277 and anti-Myc (Fig. 3a). This staining pattern was observed in all cells in which c-Myc

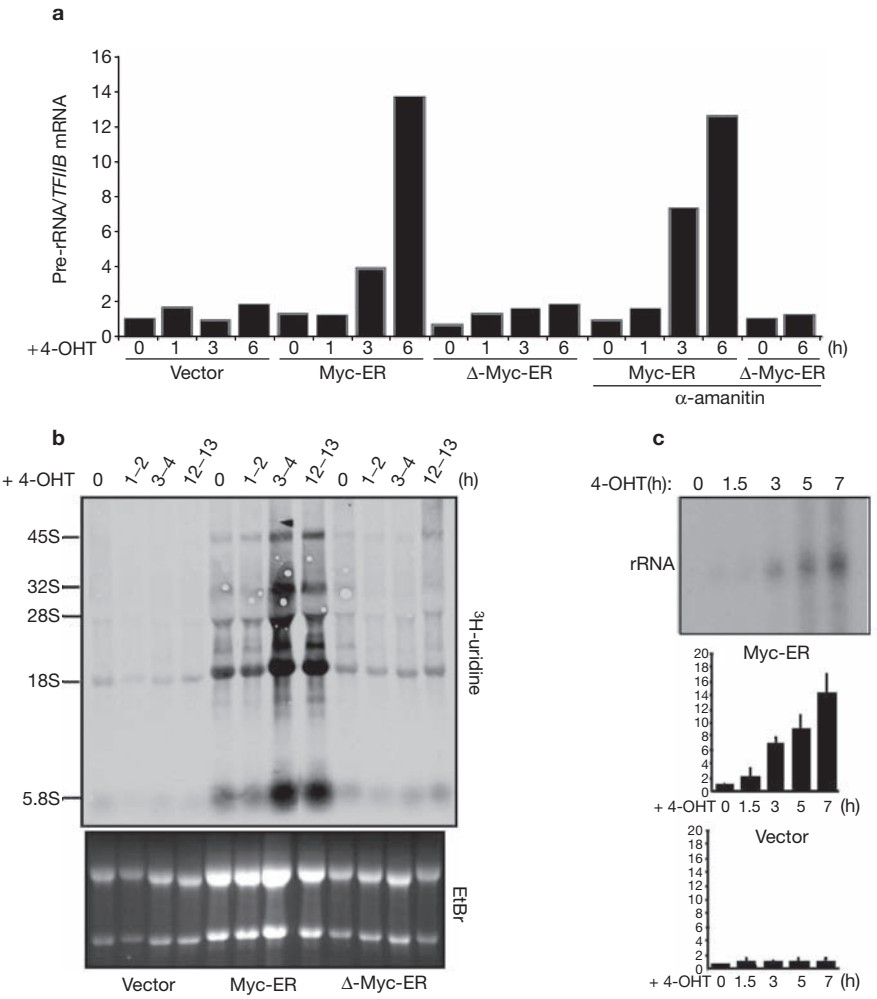

Figure 2 Analysis of pre-rRNA synthesis following Myc-ER activation. (**a**) Human primary fibroblasts (WI38) expressing the conditional Myc-ER protein, the deletion mutant Δ-Myc-ER or empty pBabe vector were cultured to quiescence and then induced with 4-hydroxy-tamoxifen (4-OHT), with or without 2 μg ml^{-1} α-amanitin, as described previously[19]. RNA was extracted at the indicated time points and analysed by reverse transcription PCR using primers specific for the 5′-ETS and for mRNA encoding TFIIB. (**b**) *In vivo* labelling with ^{3}H-uridine of cells as in **a**. For each set of viruses, samples were normalized by cell number. The higher basal levels of rRNA synthesis and accumulation in Myc-ER is due to the functional leakiness of Myc-ER. Total rRNA was visualized by ethidium bromide (EtBr) staining (**c**) Pol I transcription of linearized pMrWT template using nuclear extract (7.5 μg) prepared from Balb/c mouse fibroblasts transduced with Myc-ER, density-arrested, serum-starved and then stimulated with 4-OHT for the indicated times (in h). Quantitation shows means and standard errors (SEM) from three separate inductions. Also shown are data from parallel control experiments using cells that had been transduced with empty vector.

staining was strongly induced following serum stimulation (Fig. 3b). Although complete overlap between c-Myc and Mab 1277 is not evident (Fig. 3a,b), c-Myc is present within the nucleolar boundary that is defined by Mab1277 in this focal plane. A three-dimensional view of c-Myc and nucleoli, showing how c-Myc staining is embedded within nucleoli, was reconstructed from images collected at 0.2 μm sections throughout the nucleus (see Supplementary Information, Movies 1 and 2). In contrast to c-Myc (Fig. 3a), the transcription factor c-Jun (green) is excluded from the nucleolus, as defined by antibodies against the main rDNA binding protein, upstream binding factor (UBF), thereby producing a 'black hole' within the nucleus (Fig. 3a). The presence of c-Myc in nucleoli during the G0/G1 transition was confirmed using a different antibody against c-Myc (see Supplementary Information, Fig. S2).

To determine whether c-Myc foci in nucleoli coincide with sites of active rRNA gene transcription, we performed rRNA-FISH (fluorescence in situ hybridization) in combination with immunostaining. The experiment was carried out after serum stimulation of quiescent fibroblasts, as above. To enhance c-Myc detection in nucleoli, cells were exposed for 2 h to MG132 proteasome inhibitor, which blocks c-Myc turnover and allows its accumulation in the nucleolus[23]. Immunofluorescence with anti-Myc antibodies, anti-UBF or rabbit immunoglobulin (Ig) as control was followed by hybridization with a probe to the 5′-ETS to selectively detect nascent pre-rRNA. A substantial number of bright c-Myc-containing bright nucleolar spots (red) coincided with pre-rRNA precursors and the general pattern of c-Myc localization mirrored that of the rRNA-FISH (Fig. 3c, and see Supplementary Information,Fig. S3a). During this short treatment with MG132, the levels of pre-rRNA synthesis did not change (see Supplementary Information, Fig. S3b). As expected, anti-UBF staining, combined with rRNA-FISH performed in cells not exposed to MG132, similarly indicated colocalization with rRNA precursors (Fig. 3d). Hybridization and immunostaining specificity was monitored with a

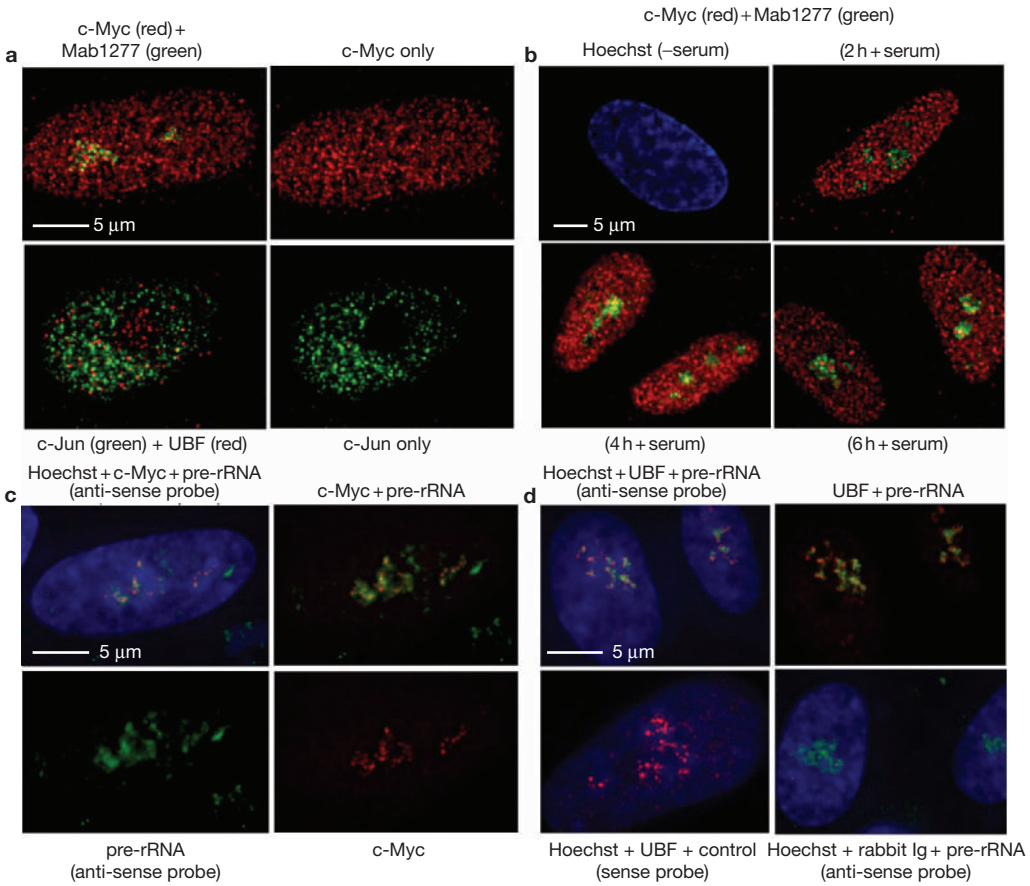

Figure 3 Endogenous c-Myc localizes in nucleoli during the G0/G1 transition. (**a**) Human TERT-immortalized human primary fibroblasts were synchronized by serum starvation and stimulated to re-enter the cycle with 10% fetal bovine serum. c-Myc staining at 2 h after serum addition (red) versus nucleoli (green) indicates the presence of bright spots in the nucleoli in marked contrast to c-Jun, which shows a 'black hole' pattern. In this case, upstream binding factor (UBF) was used as nucleolar marker (red). A projection of seven individual 0.2 μm sections is shown for both c-Myc and c-Jun; a three-dimensional view of c-Myc staining throughout the whole nucleus, reconstructed from several 0.2 μm images can be seen as a quicktime movie (see Supplementary Information, Movie 1 and 2). (**b**) Time course of c-Myc staining in cells as in **a**, indicating that following serum stimulation c-Myc is present in nucleoli, although it is barely detectable in quiescent cells. Following longer exposure, weak staining of both c-Myc and Mab1277 can be detected in quiescent cells, but after normalization with the +serum images the signal is negligible. Each image represents a single section of 0.2 μm through the nucleus. (**c**) c-Myc and UBF staining colocalizes with pre-rRNA (as in **a**). Serum-stimulated human fibroblasts (total of 4 h) were exposed to MG132 for 2 h before fixation. c-Myc staining colocalizes with pre-rRNA as detected by fluorescence *in situ* hybridization (FISH) with an antisense probe (green). (**d**) UBF staining (red) and pre-rRNA (green) is shown as positive control in cells not treated with MG132. A sense probe was used as negative control of pre-rRNA FISH; rabbit immunoglobulin (Ig) was used as negative control for the immunostaining. All images represent a single section of 0.2 μm.

rRNA sense probe and with rabbit Ig, respectively (Fig. 3d). Therefore, c-Myc localizes in nucleoli at sites of rRNA transcription.

c-Myc binds to DNA as a heterodimer with Max, enabling recognition of the E-box sequence CACGTG. Inspection of human rDNA for the presence of potential c-Myc binding sites, and of CACGTG and a variant sequence, CAC/TGCG[20], revealed several potential hexamers within rDNA genes (Fig. 4a, asterisks). A cluster of sites was detected adjacent to the transcription termination region, with 15 sites located within a 3.5-kb region of the rDNA locus, a frequency that far exceeds the calculated random distribution. To determine whether or not c-Myc is bound in vivo, we performed chromatin cross-linking and immunoprecipitation (ChIP) assays in P-493-6 cells, with either anti-c-Myc or rabbit Ig as a negative control. DNA enrichment was assayed by real-time PCR using sets of primer pairs spanning the entire human rDNA repeat[24]. Mapping of c-Myc binding throughout the rDNA locus, with a resolution of ~ 0.5–1 kb (see Fig. 4a,b) indicated that c-Myc bound to the predicted region near the transcription termination signal (H13, indicating ~13 kb from the start site, +1), with an enrichment of 10–40-fold (Fig. 4b). This enrichment was abolished following addition of Tet and c-Myc repression. We also detected c-Myc binding downstream, with primers H14 and H16 (data not shown). In addition, another peak of c-Myc binding covered a ~ 2 kb region that included the transcription initiation region (H1), the promoter (H42.9) and a region upstream of the promoter (H42) (Fig. 4b), where three potential consensus sites are located.

To investigate how c-Myc binding to rDNA loci might activate transcription, we tested the possibility that c-Myc interacts with the Pol I transcriptional machinery. Despite the high abundance of UBF in cells, we were unable to detect its co-immunoprecipitation with c-Myc (data not shown). By contrast, the much less abundant SL1 (also known as TIF-IB) was reproducibly found associated with endogenous c-Myc (Fig. 4c). SL1 is an essential complex that is composed of the TATA-binding protein (TBP) and three Pol I-specific TBP-associated factors (TAFs), TAF_I110, TAF_I63 and TAF_I48. Immunoprecipitations using antisera against TBP, TAF_I48 or TAF_I110, as well as the positive control Max,

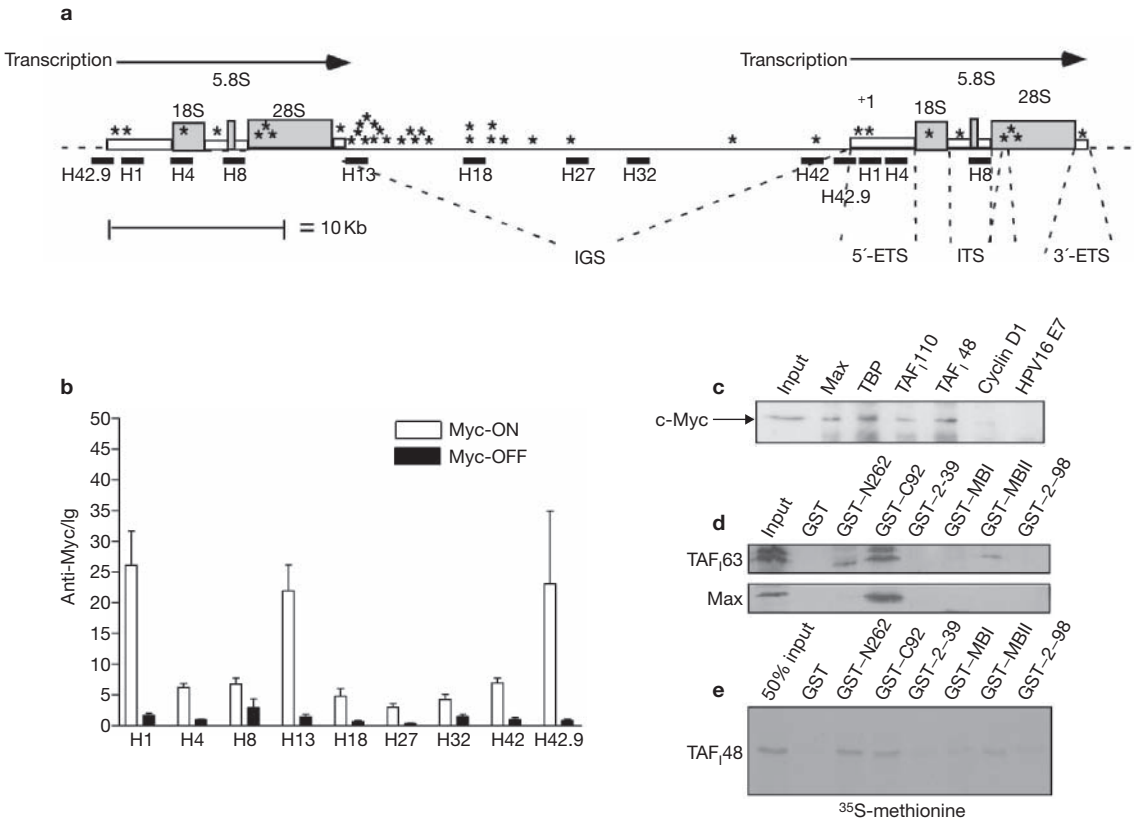

Figure 4 c-Myc binds to specific regions of human ribosomal DNA (rDNA). (**a**) Schematic representation of a human rDNA repeat with c-Myc binding sites marked by asterisks (canonical CACGTG and non-canonical CAT/CGCG). Primer pairs (solid bars) and their approximate positions relative to the transcription start are indicated. (**b**) Enrichment of rDNA obtained with anti-c-Myc versus rabbit immunoglobulin (Ig), determined by chromatin cross-linking and immunoprecipitation (ChIP) analysis using chromatin prepared from P493-6 cells with (Myc-off) or without (Myc-on) tetracycline[11]. DNA was quantitated by real-time PCR with primer sets, as indicated in **a**. Data are the means and standard error (SEM) derived from four independent ChIP experiments, each tested by at least two independent PCR reactions. (**c**) c-Myc interacts with the Pol I-specific factor SL1. Whole-cell extracts (500 μg) of human primary fibroblasts immortalized with human TERT were immunoprecipitated using antibodies against Max (H-2), TBP (MTBP-6), TAF$_I$110 (M-18), TAF$_I$48 (C-19), cyclin D1 (R-124) and HPV16 E7 (TVG710Y); precipitates were immunoblotted, alongside 10% of input, with c-Myc antibody N-262. (**d**) Pull-down assay with the indicated glutathione-*S*-transferase (GST) fusion proteins and 400 μg HeLa nuclear extract; precipitates were immunoblotted with antibodies against TAF$_I$63 and Max. (**e**) Pull-down assay with the indicated GST fusion proteins and reticulocyte lysate (2 μl) containing *in vitro* translated ^{35}S-Met-labelled TAF$_I$48.

revealed the presence of associated c-Myc (Fig. 4c). Two distinct regions of c-Myc seem to be capable of this interaction. SL1 binds strongly to a glutathione-S-transferase (GST) fusion containing the carboxy-terminal 92 residues of c-Myc, which encompasses its DNA-binding and dimerization domain, whereas an additional, weaker but specific interaction is seen with the MBII region of the amino-terminal transcription activation domain (Fig. 4d). Consistently, Pol I transcription is not induced by the Δ–*MYC-ER* mutant, and the deletion of the *Δ–MYC-ER* allele in this mutant encompasses MBII (Fig. 2). A direct interaction is suggested by the fact that the same regions of c-Myc will bind to an isolated SL1 subunit in a reticulocyte lysate (Fig. 4e).

The interaction of c-Myc with the SL1 complex indicates that c-Myc binding to rDNA may influence the occupancy of the basal Pol I transcription complex, perhaps by facilitating recruitment or stabilization. To test this, we used ChIP assays with anti-TBP antibody to monitor the presence of SL1 along the rDNA repeat in P-493-6 cells expressing Tet-Myc. This revealed a pronounced c-Myc-responsive peak (~300-fold enrichment) of SL1 binding using primer set H42.9, which amplifies the region from –57 base pair (bp) to +33 bp, including the transcription start site (+1) and the rDNA basal promoter elements (Fig. 5a). This overlaps with one of the c-Myc binding peaks, although the latter extends further, both upstream (H42) and downstream (H1) (Fig. 4b). ChIP analysis with anti-UBF antibodies indicated that UBF binds preferentially to the transcription initiation region and throughout the transcribed region, but was not detectable in the intergenic region. Repression of c-Myc by tetracycline caused a slight (~ twofold) decrease in binding of UBF around the promoter (H1 and H42.9) and a slight increase within the coding region (H4 and H8) (Fig. 5b). Binding of c-Myc to Pol II promoters is thought to enhance transcription via recruitment of histone acetylases[25]. ChIP analysis with anti-histones H3 and H4 indicated that minor peaks of histone acetylation overlapped with c-Myc binding sites that are adjacent to the transcription termination (H13) regions, as well as the initiation regions (H1). However, the main wave of histone acetylation peaked at H42 (Fig. 5c), just 1 kb upstream from the peak of TBP binding (detected at H42.9)[22]. Acetylation levels are greatly diminished following c-Myc shut-off (Fig. 5c).

Synthesis of rRNA by Pol I, which drives ribosome biogenesis, is an important determinant of the cellular growth response. We have shown

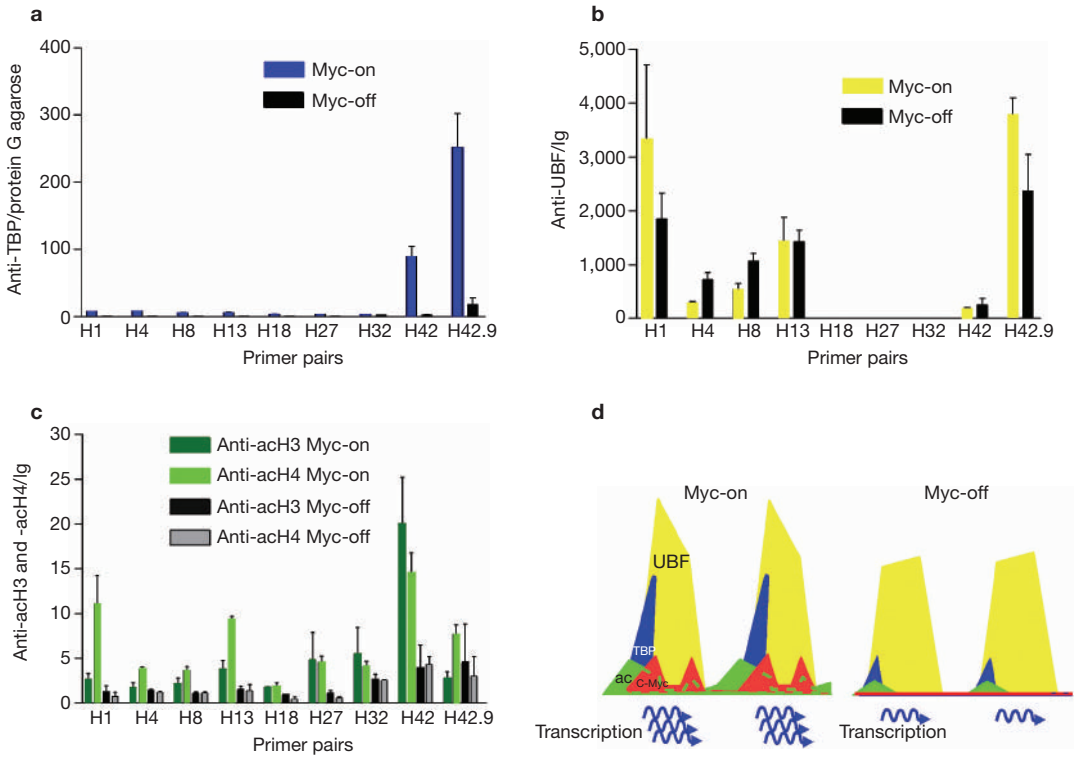

Figure 5 Changes in Pol I machinery and histone acetylation at ribosomal DNA (rDNA) in response to c-Myc. (**a**) Chromatin cross-linking and immunoprecipitation (ChIP) analysis with anti-TATA-binding protein (TBP) antibodies in P493-6 cells with c-Myc on or off. TBP binding is strictly localized to the promoter region and sharply declines following c-Myc shut-off. (**b**) Parallel analysis with anti-upstream binding factor (UBF) antibodies, indicating strong binding throughout the transcribed region but not in the intergenic region. In contrast to TBP, UBF binding is only reduced ~twofold following c-Myc shut-off at the promoter region (H1 and H42.9), whereas it increased slightly within the transcribed region. (**c**) ChIP analysis with anti-acetylated H3 and H4 antibodies (anti-acH3 and -acH4, respectively) indicates increased acetylation with c-Myc induction, starting in the upstream H32 region and peaking at H42, ~1 kb upstream of the promoter. Data for TBP and acetylation are means and SEM from a representative experiment that was analysed by at least three independent PCRs. For UBF, data are from three independent ChIP experiments. SEM are indicated. (**d**)Schematic summary of c-Myc (red), acetylation (ac, green), TBP (monitoring SL1, blue) and UBF (yellow) binding to human rDNA and changes following c-Myc shut-off.

that the oncoprotein c-Myc — a major cell growth regulator — directly influences Pol I transcription of rRNA genes. Some of the effects of c-Myc on rRNA transcription could be secondary consequences of c-Myc stimulation of other growth pathways. However, both the rapidity of the Pol I response to c-Myc and its resistance to α-amanitin indicates that a direct effect is also involved. In support of this idea, c-Myc colocalizes with nucleolar markers and with sites of rRNA transcription during the G0/G1 transition (Fig. 3). Moreover, c-Myc is associated with E-box binding sites in the rDNA promoter and terminator regions (Fig. 4) and c-Myc binding correlates with increased histone acetylation and recruitment of TBP to the rDNA promoter (summarized in Fig. 5). The latter can be explained by a physical interaction between c-Myc and the SL1 component of the basal Pol I machinery.

Two other groups have recently reported a link between c-Myc function and rRNA biosynthesis. First, Schlosser *et al.* showed that c-Myc stimulates processing of the 45S primary transcript but, in contrast to our findings, stated that there is no change in transcription of rRNA[26]. Nonetheless, their data showed increased unprocessed Pol I primary transcript when c-Myc is induced in P493-6 cells (Fig. 2c, ref. 26). Poortinga *et al.*[27] reported that c-Myc stimulates UBF transcription, thereby resulting in an increase in rRNA. We also found a modest increase in UBF associated with the rRNA promoter, but believe that direct c-Myc binding to rDNA and concomitant histone acetylation and recruitment of Pol I machinery is likely to drive rRNA transcription. In an accompanying paper (see note added in proof), Arabi *et al.* demonstrate a role for c-Myc in stimulating rRNA transcription. They propose that c-Myc turnover by ubiquitin-mediated degradation by the SKP2 ubiquitin ligase might be necessary for c-Myc to stimulate Pol I transcription, as shown for Pol II reporter genes[28]. However, we did not observe decreased synthesis of pre-rRNA after exposure to MG132 and, indeed, were able to colocalize c-Myc protein with sites of rRNA transcription (Fig. 3). In this regard, it is intriguing that the ubiquitin ligase isoform Fbw7γ, which also targets c-Myc for degradation and does not stimulate c-Myc transcriptional activity[29], is located exclusively in the nucleolus[30]. Furthermore, its knockdown leads to accumulation of c-Myc in nucleoli and increased cell growth[30]. We speculate that a nucleolar subpopulation of c-Myc, the abundance of which is determined by Fbw7γ-mediated degradation, regulates rRNA transcription during the G0/G1 transition.

Other data, from Grewal *et al.* (see note added in proof), show that the *D. melanogaster* orthologue of c-Myc (dMyc) is an important regulator of rRNA synthesis. Therefore, the control of rRNA synthesis is an evolutionarily conserved c-Myc function. However, dMyc seems to stimulate rRNA transcription indirectly, by inducing components of the Pol I machinery. This indicates that, during evolution, vertebrate c-Myc has acquired a direct mechanism of rRNA regulation, perhaps reflecting tighter coupling of growth with proliferation in vertebrate cells.

It is intriguing that c-Myc binds within both the rDNA promoter and terminator regions (Figs 4, 5). The recent crystal structure of c-Myc–Max bound to E-box DNA demonstrated that the c-Myc–Max heterodimers can themselves dimerize to form a bivalent heterotetramer[31]. A c-Myc–Max tetramer may have the potential to spatially juxtapose rRNA terminator and initiator elements. Indeed, it has been suggested that looping within the rDNA locus facilitates rRNA transcription[32].

In contrast to positive regulation of Pol I transcription by c-Myc, the tumour suppressors RB, p53 and ARF exert negative control of rRNA production (see refs 1,33 for reviews). So, deregulating the opposing activities that control rRNA synthesis may accompany tumour formation. Our data on c-Myc activation of Pol I transcription, together with previous reports on c-Myc regulation of Pol II and Pol III, indicate that the profound effects of c-Myc on several aspects of cellular function involve a capacity to directly influence transcription by all three nuclear RNA polymerases.

Note added in proof: accompanying manuscripts by Grewal, S. S. et al. *(*Nature Cell Biol. **7,** *295–302 (2005)) and Arabi* et al. *(*Nature Cell Biol. **7,** *303–310 (2005)) are published in this issue.*

METHODS

Cell cultures and retroviral vectors. Human primary foreskin fibroblasts or WI38 cells were cultured in DMEM media and transduced with retroviral vectors expressing *c-MYC* (pB-Myc), *DDX18* (ref. 20), a dominant-negative DDX18 mutant with a lysine to alanine substitution in the DEAD-box domain, or empty retroviral vector pBabe. Cells were selected in puromycin and used for labelling experiments within 2–4 passages after selection. For the Myc-ER experiments, WI38 were transduced with *pB-MYC-ER* or Δ*-MYC-ER* (deletion 106–143 (ref. 21)). Cells were density-arrested and serum-starved before induction with 4-hydroxy-tamoxifen (4-OHT). Wild-type and *c-MYC*$^{-/-}$ fibroblasts were cultured as described previously[9].

Transcription analysis. rRNA precursors were analysed by labelling cells with either ^{3}H-uridine or ^{3}H-methyl-methionine, as described previously[34]. At the indicated time points, cells were washed in cold phosphate-buffered saline (PBS) once and lysed in Trizol for RNA isolation. RNA was separated on 1% agarose-formaldehyde gels, transferred to nylon membranes and sprayed with EN^{3}HANCE (#NEF970; PerkinElmer, Boston, MA) before carrying out autoradiography.

Reverse transcription PCR (RT-PCR) of human pre-rRNA used primers 5′-CCTGCTGTTCTCTCGCGCGTCCGAG-3′ and 5′-AACGCCTGACACGCACGGCACGGAG-3′; for rat pre-rRNA, primers used were 5′-TCGCGCTCCTTACCTGG-3′ and 5′-CGGCATGTATTAGCTCTA-3′; in both cases, cycling parameters were 95 °C for 3 min, followed by 25 cycles of [95 °C for 1 min, 65 °C for 1 min, 72 °C for 1 min] and then 72 °C for 5 min. RT-PCR of 5S rRNA and ARPP P0 mRNA was conducted as described previously[19]. RT-PCR of TFIIB mRNA used primers 5′-CAGTTGTAATCAAATCCACAC-3′ and 5′-GCAGACAGAATCAATCTAC-3′; cycling parameters were 95 °C for 3 min, followed by 20 cycles of [95 °C for 30 s, 57 °C for 30 s, 72 °C for 30 s] and then 72 °C for 5 min.

Run-on assays were performed with P-493-6 cells, collected either in the presence of tetracycline or following release after 4 and 8 h. Approximately 10^{8} cells were lysed in hypotonic buffer containing 0.5% NP40 and nuclei were washed in nuclear buffer as described previously[20]. Nuclei were resuspended in 50 mM Tris pH 8, 5 mM $MgCl_2$, 40% glycerol, 1 mM DTT and then frozen. Nascent RNAs were labelled, after adjusting to 150 mM KCl, by the addition of nucleoside triphosphates and α-^{32}P cytidine-triphosphate. Nuclei were incubated at 30 °C for 30 min, treated with DNAse I, followed by proteinase K digestion. Nuclear RNA was extracted using Trizol (Invitrogen, Carlsbad, CA) and resuspended in hybridization buffer. Plasmid probes for rRNA corresponded to the 5′-ETS (+414 to +700) and 28S human sequences, whereas human cDNAs for *MYC*, *MAX* and *TUBULIN* were used for controls.

In vitro transcription monitored synthesis by nuclear extracts of radiolabelled run-off transcripts from pMrWT, which contains mouse rRNA gene sequences from –169 to +155; the plasmid was linearized with EcoR1 at +158 and reactions were conducted as described previously[19].

Immunofluorescence and FISH. Human TERT-immortalized fibroblasts were routinely used for the immunofluorescence experiments to detect endogenous c-Myc. Cells were plated on coverslips and cultured to confluency for at least 1 week, then serum-starved in 0.1% fetal calf serum (FCS) for 72 h and re-stimulated with complete media containing 10% FCS for the indicated times. For immunofluorescence, cells were fixed in 4% paraformaldehyde (#15710; Electron Microscopy Sciences, Hatfield, PA) for 10 min at room temperature, permeabilized in PBS/0.5% Triton X-100 for 5 min on ice, then incubated with the primary antibodies for 1–2 h at 37 °C. The following primaries were used: anti-c-Myc 1:50 (# 764; Santa Cruz Biotechnology, Santa Cruz, CA); anti-UBF 1: 100 (#9131; Santa Cruz); anti-nucleoli 1: 50 (Mab 1277; Chemicon International, Temecula, CA); anti-c-Jun 1: 50 (#822; Santa Cruz). Coverslips were washed and incubated with secondary antibodies 1:1000 (Rhodamine or Fluorescein AffiPure goat anti-rabbit or anti-mouse IgG, respectively; Jackson Immuno Research, West Grove, PA). Hoechst was included to visualize nuclei. Coverslips were mounted with Vectashield (Vector Laboratories, Burlingame, CA). Pictures were taken with a ×100 objective with an Olympus IX70 inverted microscope by wide-field epi-flourescence deconvolution microscopy (Delta Vision, Applied Precision, Issaquah, WA). The exposure times were kept constant for each fluorescence channel within each experiment and antibody was used. Images were taken at each 0.2 μm section through the nucleus, and generally 40 sections per field were collected. Selected sections are shown as specified in the figure legends. Images were deconvolved using SoftWoRx 2.5 software from Applied Precision. For rRNA-FISH analysis, cells were first subjected to immunofluorescence as above, post-fixed in 4% paraformaldehyde and then hybridized with a 5′-ETS (spanning from +414 to +700) antisense or sense probe cloned into pCS-2 and transcribed using DIG RNA labelling mix (Enzo Biochem, Farmingdale, NY). Hybridizations were carried out at 65 °C in the presence of 50% formamide and 2X SSC overnight. After washing (two times in 2X SSC at 37°C, two times in 2X SSC and once in 1X SSC at room temperature), the coverslips were incubated with anti-digoxigenin-fluorescein Fab fragments for 1 h at 37°C and washed four times in 4X SSC and 0.025% Tween 20 (Hoechst was included during the third wash). Mounting was in Vectashield, as above.

Chromatin cross-linking and immunoprecipitation (ChIP) analysis. P493-6 cells[11] expressing *Tet-MYC* were grown without (Myc-on) or with (72 h, Myc-off) tetracycline in RPMI media with 10% fetal bovine serum. For crosslinking, ~ 10^{8}–10^{9} cells were resuspended in 50 ml warm medium containing 1% formaldehyde for 10 min at room temperature. Cells were lysed in 1–3 ml of 1% SDS, 50 mM Tris pH 8, 10 mM EDTA, 10 mM Na Butyrate and protease inhibitor cocktail (Roche Diagnostics, Mannheim, Germany) and sonicated seven times for 15 s to achieve a chromatin size of 100–500 bp. ChIP antibodies were for c-Myc (#764; Santa Cruz), for UBF (#9131; Santa Cruz), for acetylated histone H3 (#06-599; Upstate Biotechnologies, Waltham, MA), for acetylated histone H4 (#06-866; Upstate) and for TBP (MTBP-6).

Equal numbers of cells (~ 2–5 × 10^{7}) were used for each immunoprecipitation (details available on request) and the extracted DNA for each immunoprecipitation was resuspended in 25–75 μl of TE (10 mM Tris pH 8, 1 mM EDTA). In parallel, an input DNA sample was prepared and resuspended in 100 μl TE. Real-time PCR was used to quantitate the immunoprecipitated DNA relative to a standard curve built with 1 μl of input dilutions. The fold enrichment was calculated relative to the background detected with non-specific rabbit Ig or prG for each primer set, as indicated in the figures. PCR conditions using SYBR GREEN mix (#4309155, Applied Biosystems, Foster City, CA) for all primers were as follows: 96 °C × 2 min, followed by 45 cycles at 96 °C for 30 s, 58 °C for 1 min. Primers were derived from ref. 24, with a few exceptions. Sequence of the primers can be found in Supplementary Information, Table S1.

RNA interference. In Fig. 1f, growing HeLa cells were transfected using siPORTlipid (Ambion, Austin, TX) according to the manufacturer's protocol, with siRNAs against c-Myc or glyceraldehyde-3-phosphate dehydrogenase that were purchased from Ambion. Fig. 1g used pSUPER vectors carrying siRNAs against c-Myc or lamin that were obtained from the Cancer Research UK siRNA library. These were transfected in optiMEM (GibcoBRL, Paisley, UK) using lipofectamine (Invitrogen, Paisley, UK). RNA and protein were harvested 24 h (Fig. 1f) or 48 h (Fig. 1g) after transfection.

Pull-down and co-immunoprecipitation. Pull-down assays were carried out as described previously[19], with HeLa cell nuclear extract or reticulocyte lysate containing ^{35}S-Met-labelled TAF_I48. GST fusion proteins contained the following c-Myc residues: GST-N262, residues 1–262; GST-C92, residues 347–439; GST-2-39, residues 2–39; GST-MBI, residues 40–98; GST-MBII, residues 99–156; GST-2-98, residues 2–98.

Co-immunoprecipitations were carried out as previously described[19]. TAF_I63 and MTBP-6 antibodies were from L. Comai and J. Flint, respectively. Other antibodies were from Santa Cruz Biotechnologies.

BIND identifiers. Seven BIND identifiers (www.bind.ca) are associated with this manuscript: 197248, 197249, 197250, 197242, 197243, 197244 and 197245.

Note: Supplementary Information is available on the Nature Cell Biology website.

ACKNOWLEDGEMENTS

We thank L. Comai and J. Flint for generous gifts of antibodies and A. Burdick and K. Robinson for technical assistance; J. Benanti, M. Welcker and B. Moorefield for critical reading of the manuscript; T. Ragoczy, S. Kosak, M. Lorincz and D. Dickerson in the Groudine laboratory for advice on FISH and run-on assays; T. Sawado for the ChIP protocol; and the Fred Hutchinson Image Analysis staff for help with DeltaVision microscopy. We are also grateful to R. Reeder for helpful discussions during the course of this work. Support for this work was from National Institutes of Health grants to C.G. D.A.G. and R.N.E.; and Cancer Research UK grants to R.J.W. R.N.E. is an American Cancer Society Research professor.

COMPETING FINANCIAL INTERESTS

The authors declare that they have no competing financial interests.

Received 10 November 2004; accepted 22 December 2004
Published online at http://www.nature.com/naturecellbiology.

1. Grummt, I. Life on a planet of its own: regulation of RNA polymerase I transcription in the nucleolus. *Genes Dev.* **17,** 1691–1702 (2003).
2. Dang, C. V. c-Myc target genes involved in cell growth, apoptosis, and metabolism. *Mol. Cell. Biol.* **19,** 1–11 (1999).
3. Grandori, C., Cowley, S. M., James, L. P. & Eisenman, R. N. The Myc/Max/Mad network and the transcriptional control of cell behavior. *Annu. Rev. Cell. Dev. Biol.* **16,** 653–699 (2000).
4. Lutz, W., Leon, J. & Eilers, M. Contributions of Myc to tumorigenesis. *Biochim. Biophys. Acta* **1602,** 61–71 (2002).
5. Eilers, M., Picard, D., Yamamoto, K. R. & Bishop, J. M. Chimaeras of myc oncoprotein and steroid receptors cause hormone-dependent transformation of cells. *Nature* **340,** 66–68 (1989).
6. Johnston, L. A., Prober, D. A., Edgar, B. A., Eisenman, R. N. & Gallant, P. *Drosophila* myc regulates cellular growth during development. *Cell* **98,** 779–790 (1999).
7. Trumpp, A. *et al.* c-Myc regulates mammalian body size by controlling cell number but not cell size. *Nature* **414,** 768–773 (2001).
8. Knoepfler, P. S., Cheng, P. F. & Eisenman, R. N. N-myc is essential during neurogenesis for the rapid expansion of progenitor cell populations and the inhibition of neuronal differentiation. *Genes Dev.* **16,** 2699–2712 (2002).
9. Mateyak, M. K., Obaya, A. J., Adachi, S. & Sedivy, J. M. Phenotypes of c-Myc-deficient rat fibroblasts isolated by targeted homologous recombination. *Cell Growth Differ.* **8,** 1039–1048 (1997).
10. Iritani, B. M. & Eisenman, R. N. c-Myc enhances protein synthesis and cell size during B lymphocyte development. *Proc. Natl Acad. Sci. USA* **96,** 13180–13185 (1999).
11. Schuhmacher, M. *et al.* Control of cell growth by c-Myc in the absence of cell division. *Curr. Biol.* **9,** 1255–1258 (1999).
12. Pierce, S.B. *et al.* dMyc is required for larval growth and endoreplication in *Drosophila*. *Development* **131,** 2317–2327 (2004).
13. Coller, H. A. *et al.* Expression analysis with oligonucleotide microarrays reveals that Myc regulates genes involved in growth, cell cycle, signaling, and adhesion. *Proc. Natl Acad. Sci. USA* **97,** 3260–3265 (2000).
14. Guo, Q. M. *et al.* Identification of c-myc responsive genes using rat cDNA microarray. *Cancer Res.* **60**, 5922–5928 (2000).
15. Boon, K. *et al.* N-myc enhances the expression of a large set of genes functioning in ribosome biogenesis and protein synthesis. *EMBO J.* **20,** 1383–1393 (2001).
16. Shiio, Y. *et al.* Quantitative proteomic analysis of Myc oncoprotein function. *EMBO J.* **21,** 5088–5096 (2002).
17. Orian, A. *et al.* Genomic binding by the *Drosophila* Myc, Max, Mad/Mnt transcription factor network. *Genes Dev.* **17,** 1101–1114 (2003).
18. Fernandez, P. C. *et al.* Genomic targets of the human c-Myc protein. *Genes Dev.* **17,** 1115–1129 (2003).
19. Gomez-Roman, N., Grandori, C., Eisenman, R. N. & White, R. J. Direct activation of RNA polymerase III transcription by c-Myc. *Nature* **421,** 290–294 (2003).
20. Grandori, C., Mac, J., Siebelt, F., Ayer, D. E. & Eisenman, R. N. Myc–Max heterodimers activate a DEAD box gene and interact with multiple E box-related sites *in vivo*. *EMBO J.* **15,** 4344–4357 (1996).
21. Littlewood, T. D., Hancock, D. C., Danielian, P. S., Parker, M. G. & Evan, G. I. A modified oestrogen receptor ligand-binding domain as an improved switch for the regulation of heterologous proteins. *Nucleic Acids Res.* **23,** 1686–1690 (1995).
22. Gonzalez, I. L. & Sylvester, J. E. Complete sequence of the 43-kb human ribosomal DNA repeat: analysis of the intergenic spacer. *Genomics* **27,** 320–328 (1995).
23. Arabi, A., Rustum, C., Hallberg, E. & Wright, A. P. Accumulation of c-Myc and proteasomes at the nucleoli of cells containing elevated c-Myc protein levels. *J. Cell Sci.* **116,** 1707–1717 (2003).
24. O'Sullivan, A. C., Sullivan, G. J. & McStay, B. UBF binding *in vivo* is not restricted to regulatory sequences within the vertebrate ribosomal DNA repeat. *Mol. Cell. Biol.* **22,** 657–668 (2002).
25. McMahon, S. B., Wood, M. A. & Cole, M. D. The essential cofactor TRRAP recruits the histone acetyltransferase hGCN5 to c-Myc. *Mol. Cell. Biol.* **20,** 556–562 (2000).
26. Schlosser, I. *et al.* A role for c-Myc in the regulation of ribosomal RNA processing. *Nucleic Acids Res.* **31,** 6148–6156 (2003).
27. Poortinga, G. *et al.* MAD1 and c-Myc regulate UBF and rDNA transcription during granulocyte differentiation. *EMBO J.* **23,** 3325–3335 (2004).
28. von der Lehr, N. *et al.* The F-box protein Skp2 participates in c-Myc proteosomal degradation and acts as a cofactor for c-Myc-regulated transcription. *Mol. Cell* **11,** 1189–1200 (2003).
29. Welcker, M. *et al.* The Fbw7 tumor suppressor regulates glycogen synthase kinase 3 phosphorylation-dependent c-Myc protein degradation. *Proc. Natl Acad. Sci. USA* **101,** 9085–9090 (2004).
30. Welcker, M., Orian, A., Grim, J. A., Eisenman, R. N. & Clurman, B. E. A nucleolar isoform of the Fbw7 ubiquitin ligase regulates c-Myc and cell size. *Curr. Biol.* **14,** 1852–1857 (2004).
31. Nair, S. K. & Burley, S. K. X-ray structures of Myc-Max and Mad-Max recognizing DNA. Molecular bases of regulation by proto-oncogenic transcription factors. *Cell* **112,** 193–205 (2003).
32. Kulkens, T., van der Sande, C. A., Dekker, A. F., van Heerikhuizen, H. & Planta, R. J. A system to study transcription by yeast RNA polymerase I within the chromosomal context: functional analysis of the ribosomal DNA enhancer and the RBP1/REB1 binding sites. *EMBO J.* **11,** 4665–4674 (1992).
33. White, R. J. RNA Polymerase I and III, growth control and cancer. *Nature Rev. Mol. Cell Biol.* **6,** 69–79 (2005).

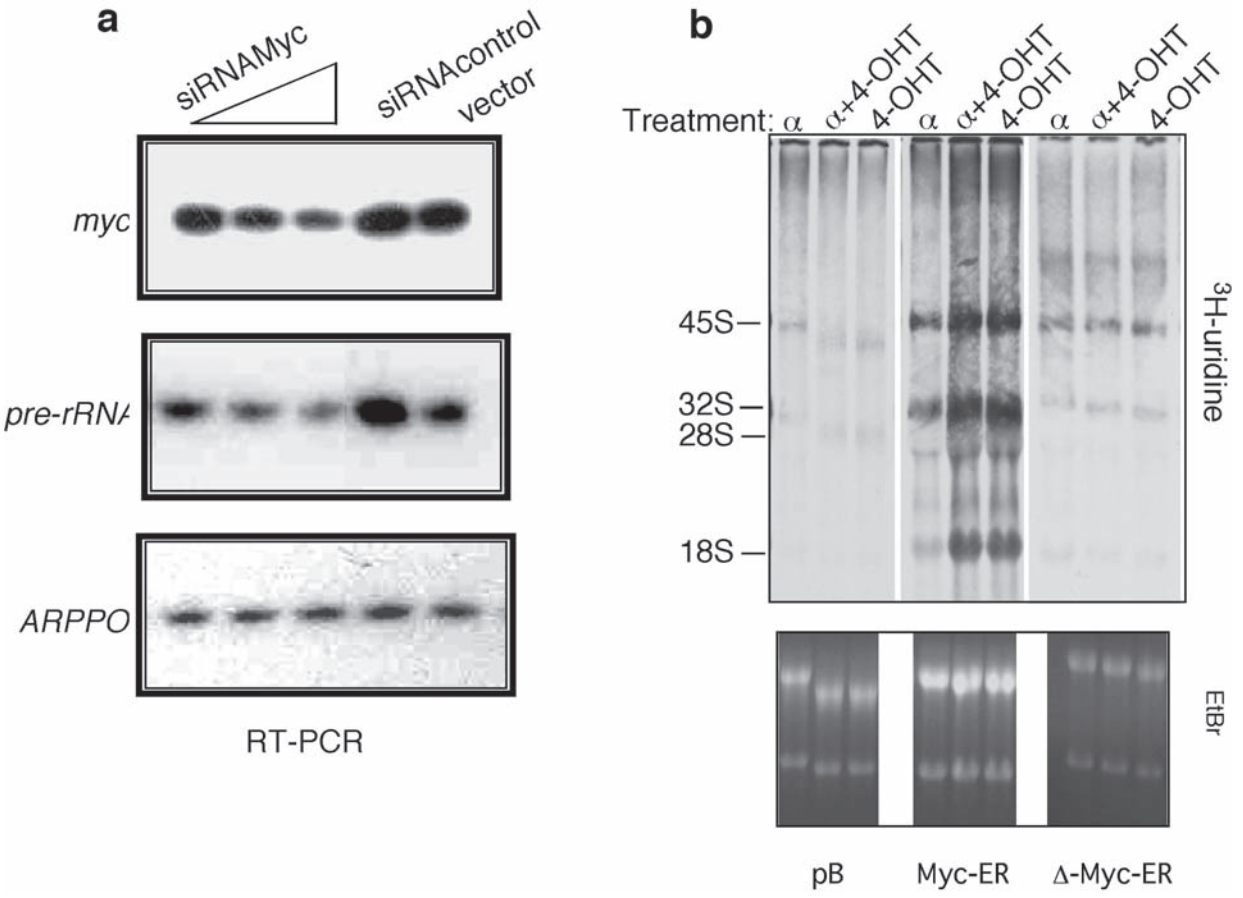

Figure S1 rRNA synthesis correlates with c-Myc levels and it is induced independently of Pol II transcription. **a)** Dose-dependent inhibition of pre-rRNA expression by titration of *c-myc* siRNA. HeLa cells were transfected with siRNAMyc#1 to a final concentration of 20nM, 30nM or 50nM (lanes 1-3, respectively), with 50nM control siRNA against GAPDH (lane 4) or with transfection mix alone in the absence of siRNA (lane 5). **b)** Effect of α-amanitin on rRNA synthesis as detected by 3H-uridine labeling of WI38 cells expressing Myc-ER, Δ-Myc-ER or empty retroviral vector. Induction of rRNA synthesis, monitored after 3hr of 4-OHT addition by labeling cells for 1hr, occurs only in Myc-ER expressing cells and it is resistant to addition of α-amanitin.

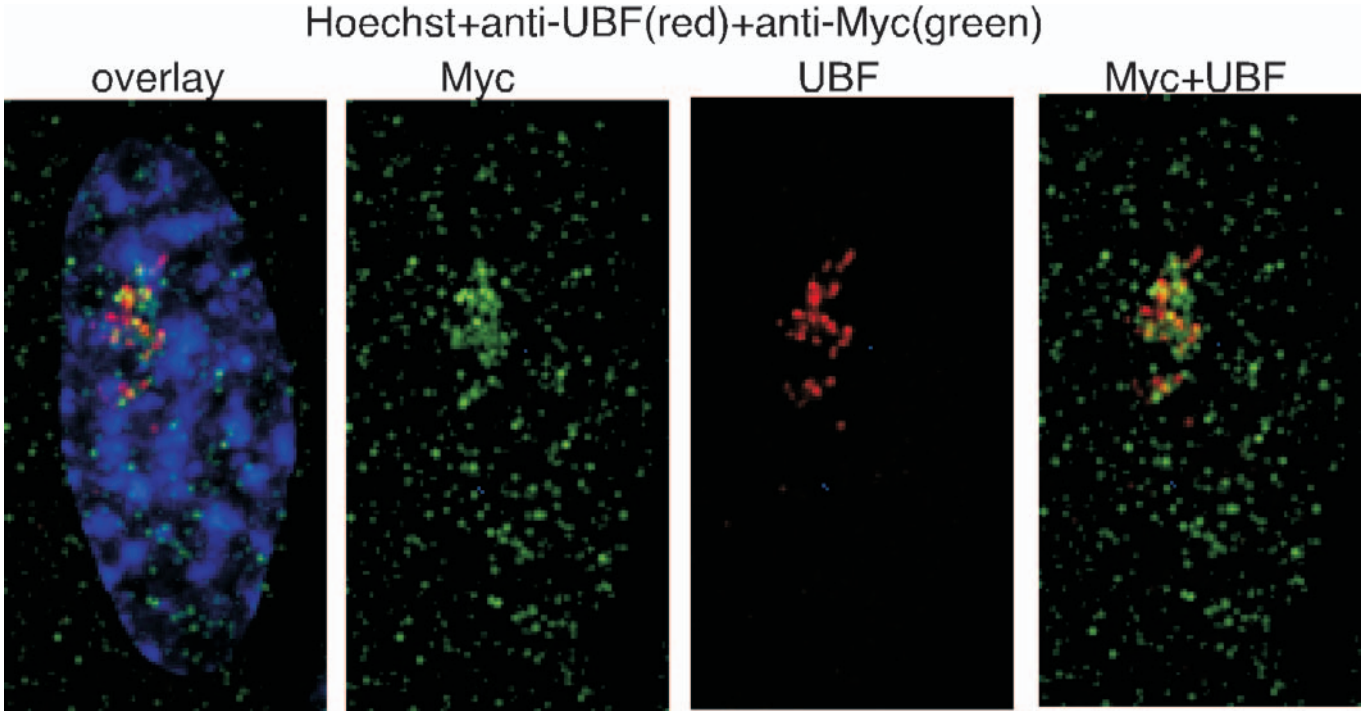

Figure S2 c-Myc localized in nucleoli as defined by anti-UBF staining during G0-G1 transition. c-Myc and UBF co-staining. H-TERT immortalized fibroblasts were serum stimulated after quiescence and fixed at 4 hr after serum addition. Anti-UBF (red; Santa Cruz#9131) shows a clear enrichment in nucleoli, where also some c-Myc staining, detectable using the monoclonal antibody 9E10 (Santa Cruz), partially overlaps with UBF. The images represent a single section of 0.2μ through the nucleolus.

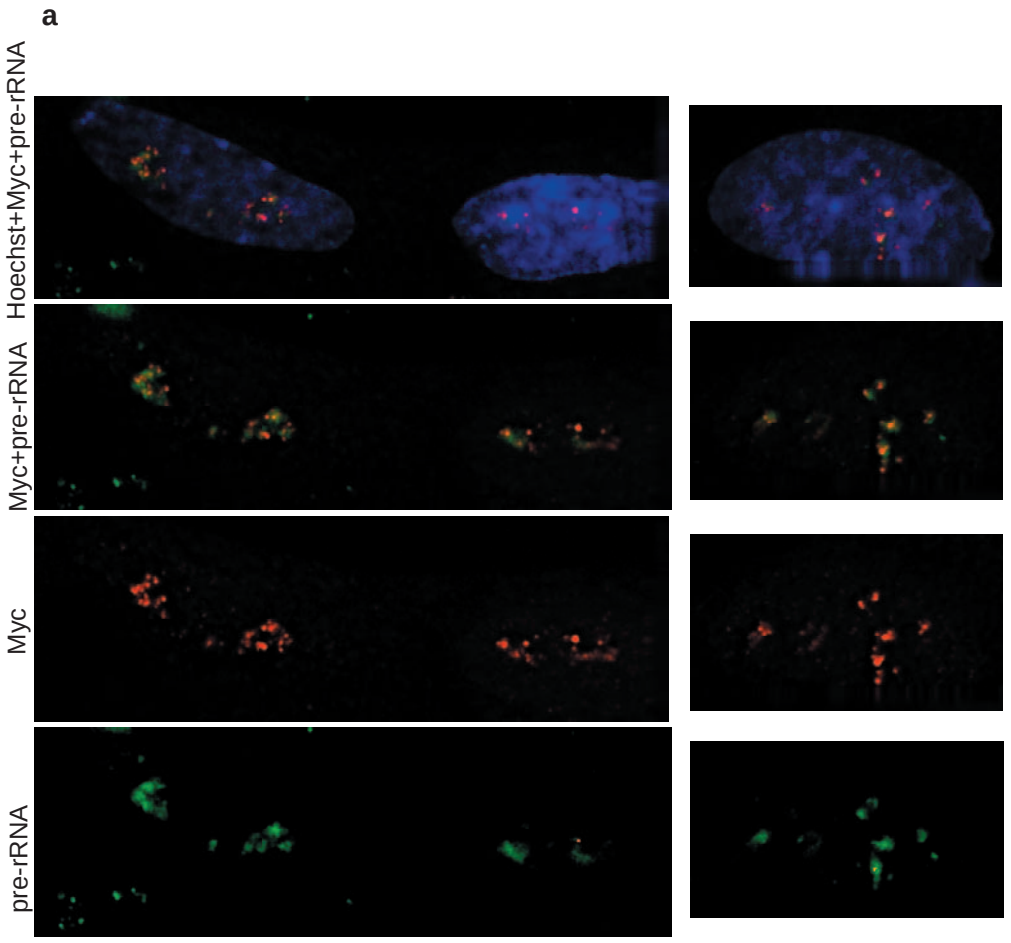

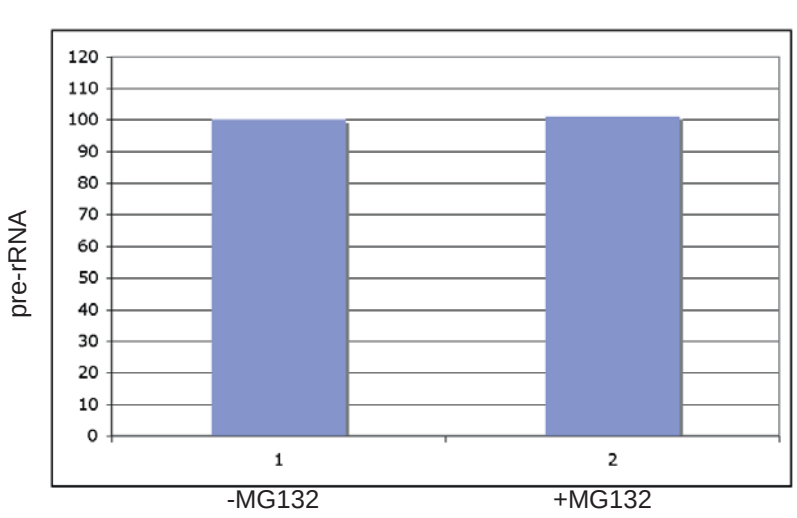

Figure S3 Immuno-rRNA FISH indicating that c-Myc co-localizes with sites of pre-rRNA transcription**. a)** Additional pictures of c-Myc staining co-localizing with pre-rRNA. H-Tert immortalized fibroblasts were arrested by serum starvation for 72 hr and then restimulated with 10% serum for 4 hr. MG132 was added at 40μM, 2hr prior to fixation. Under these conditions endogenous c-Myc is predominantly nucleolar and pre-rRNA synthesis is not inhibited as shown below. **b)** Short term MG132 treatment does not affect synthesis of pre-rRNA. H-TERT immortalized fibroblasts treated as above were collected for RNA analysis. Quantitation of pre-rRNA from equal number of cells was obtained by real time PCR of cDNA obtained with primers specific for the ITS-1 (internal transcribed spacer-1 from +6039 to +6166, Genbank #U13369) region. The average of two independent experiments is shown.

Table S1 List of all primers used to detect rDNA in ChIP experiments, nucleotide position is according to the rDNA sequence from Genbank accession #U13369

	forward	reverse	amplified region	product size
H1	GGCGGTTTGAGTGAGACGAGA	ACGTGCGCTCACCGAGAGCAG	952 to 1030	78
H4	CGACGACCCATTCGAACGTCT	CTCTCCGGAATCGAACCCTGA	3990 to 4092	102
H8	AGTCGGGTTGCTTGGGAATGC	CCCTTACGGTACTTGTTGACT	8204 to 8300	96
H13	ACCTGGCGCTAAACCATTCGT	GGACAAACCCTTGTGTCGAGG	12855 to 12970	115
H18	GTTGACGTACAGGGTGGACTG	GGAAGTTGTCTTCACGCCTGA	18155 to 18280	125
H27	CCTTCCACGAGAGTGAGAAGCG	CTCGACCTCCCGAAATCGTACA	27366 to 27477	111
H32	GGAGTGCGATGGTGTGATCT	TAAAGATTAGCTGGGCGTGG	32734 to 32859	125
H42	AGAGGGGCTGCGTTTTCGGCC	CGAGACAGATCCGGCTGGCAG	41982 to 42075	93
H42.9	CCCGGGGGAGGTATATCTTT	CCAACCTCTCCGACGACA	42943 to 33	89

Primer pairs used in ChIP experiments. The position is relative to the transcription start site at +1

Movie 1 c-Myc is not excluded from nucleoli of cells during G0-G1 transition. This is by the homogenous staining pattern in the nucleus reconstructed in 3-D with the Volocity software (Improvision). In order to visualize the whole nucleus, images obtained from ~40 individual sections at 0.2 µm intervals were utilized to recreate this image.
Movie 2 c-Myc is embedded within the nucleoli. The nucleolus from the same cell of movie 1 stained with Mab1277 (green) indicates that Myc (red) is present in the same focal planes of this nucleolar marker.

siRNA sequences

The sequences of the c-Myc siRNAs from Ambion are as follows:-

Sense: CGAUUCCUUCUAACAGAAAtt

Antisense: UUUCUGUUAGAAGGAAUCGtt

BLAST search analyses indicate that besides c-Myc, these sequences are also expressed by the human gene for lysophospholipase 1 (also called acyl protein thioesterase 1). This suggests that although specificity is high, it is not absolute. Since the additional target is a membrane protein and is not believed to be involved directly in gene expression, its potential knockdown is unlikely to contribute to the observed transcriptional responses.